

NASA TECHNICAL NOTE

NASA TN D-2743



AMPTIAC

59654

DISTRIBUTION STATEMENT A
Approved for Public Release
Distribution Unlimited

copy

STUDIES OF FATIGUE CRACK GROWTH
IN ALLOYS SUITABLE FOR
ELEVATED-TEMPERATURE APPLICATIONS

by C. Michael Hudson

Langley Research Center
Langley Station, Hampton, Va.

Reproduced From
Best Available Copy

NASA TN D-2743

STUDIES OF FATIGUE CRACK GROWTH IN ALLOYS SUITABLE FOR
ELEVATED-TEMPERATURE APPLICATIONS

By C. Michael Hudson

Langley Research Center
Langley Station, Hampton, Va.

20011130 134

NATIONAL AERONAUTICS AND SPACE ADMINISTRATION

For sale by the Office of Technical Services, Department of Commerce,
Washington, D.C. 20230 -- Price \$1.00

STUDIES OF FATIGUE CRACK GROWTH IN ALLOYS SUITABLE FOR
ELEVATED-TEMPERATURE APPLICATIONS

By C. Michael Hudson
Langley Research Center

SUMMARY

Constant-amplitude axial-load fatigue-crack-propagation tests were conducted on 8-inch (20.3-cm) wide sheet specimens made of AM 350 (CRT) and AM 367 stainless steels, two thicknesses of Ti-8Al-1Mo-1V (duplex annealed) titanium alloy, 2020-T6, 2024-T81 (clad), and RR-58 (clad) aluminum alloys, and Inconel 718 superalloy. Tests were conducted at room, elevated, and cryogenic temperatures to determine the effect of temperature on crack propagation in each material.

The fatigue-crack-growth resistance of the materials was determined and compared with materials tested similarly in a previous investigation. At elevated temperature, the 0.050-inch (1.27-mm) thick titanium alloy, Ti-8Al-1Mo-1V, in either the duplex- or triplex-annealed condition showed the greatest resistance to crack growth. At the room and cryogenic temperatures, the superalloy Inconel 718 appeared to be the most resistant. The AM 367 stainless steel showed good resistance to crack growth at all temperatures but only a limited number of tests were conducted on this material.

INTRODUCTION

A study of the fatigue-crack-growth characteristics of nine materials having potential use in supersonic aircraft is reported in reference 1 which is extended herein to include seven additional materials. Axial-load fatigue tests were conducted at positive mean stresses on 8-inch (20.3-cm) wide sheet specimens. Identical tests were conducted at elevated, room, and cryogenic temperatures to determine the effect of temperature on fatigue crack growth.

The experimental results of this study are presented in this paper. The effects of temperature on crack propagation in each material were determined. In addition, the crack-growth characteristics of the seven materials tested are compared with the characteristics of the most resistant materials tested in the previous investigation (ref. 1) to provide a comprehensive ranking of each material with respect to resistance to fatigue crack propagation.

SYMBOLS

The units used for the physical quantities defined in this paper are given both in the U.S. Customary Units and in the International System of Units (SI). Factors relating the two systems are given in reference 2.

- a one-half of the total length of a central symmetrical crack, inches or centimeters (cm)
- N number of cycles
- S_a alternating stress amplitude, ksi or meganewton/meter² (MN/m²)
- S_m mean stress, ksi or meganewtons/meter² (MN/m²)
- t specimen thickness, inch or millimeters (mm)

TESTS

Specimens

The materials tested in this investigation are listed in the following table:

Material	Condition	Thickness	
		in.	mm
Stainless steel	AM 350 (CRT)	0.050	1.27
Stainless steel	AM 367	.050	1.27
Aluminum alloy	2020-T6	.050	1.27
Aluminum alloy	2024-T81 (clad)	.063	1.61
Aluminum alloy	RR-58 (clad)	.063	1.61
Titanium alloy	Ti-8Al-1Mo-1V (duplex annealed)	.050	1.27
Titanium alloy	Ti-8Al-1Mo-1V (duplex annealed)	.250	6.35
Superalloy	Inconel 718	.050	1.27

All the specimens for each alloy were obtained from the same mill heat. The tensile properties of each material tested are listed in table I and the nominal chemical compositions, in table II.

The general configuration of the specimens may be seen in figure 1. The specimens were 24 inches (61 cm) long and 8 inches (20.3 cm) wide. All specimens were made with the longitudinal axis of the specimens parallel to the

grain of the sheet. A 0.1-inch (0.254-cm) notch was cut into the center of each specimen by means of an electrical discharge process. Very localized heating occurs in making notches in this manner. Thus, virtually all of the material through which the fatigue crack propagates is unaltered by the cutting process.

Prior to shearing the specimen blanks, the sheet materials were covered with tape to protect the surfaces. Following shearing, all specimens were chemically cleaned. Those specimens requiring heat treatment were then heat treated according to the procedures outlined in table III.

A reference grid (fig. 2) was photographically printed on the specimen surfaces to define intervals along the crack path. This photographic method produces no mechanical defects in the specimen surface, and, consequently, no stress concentrations are introduced. Metallographic examination and tensile tests conducted on specimens bearing the grid indicate that the grid had no detrimental effects upon the materials tested.

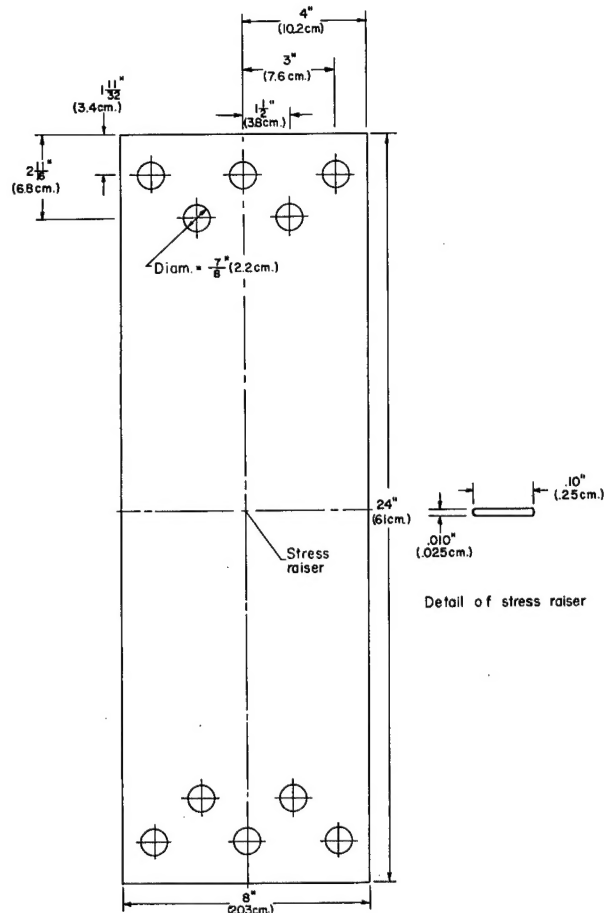
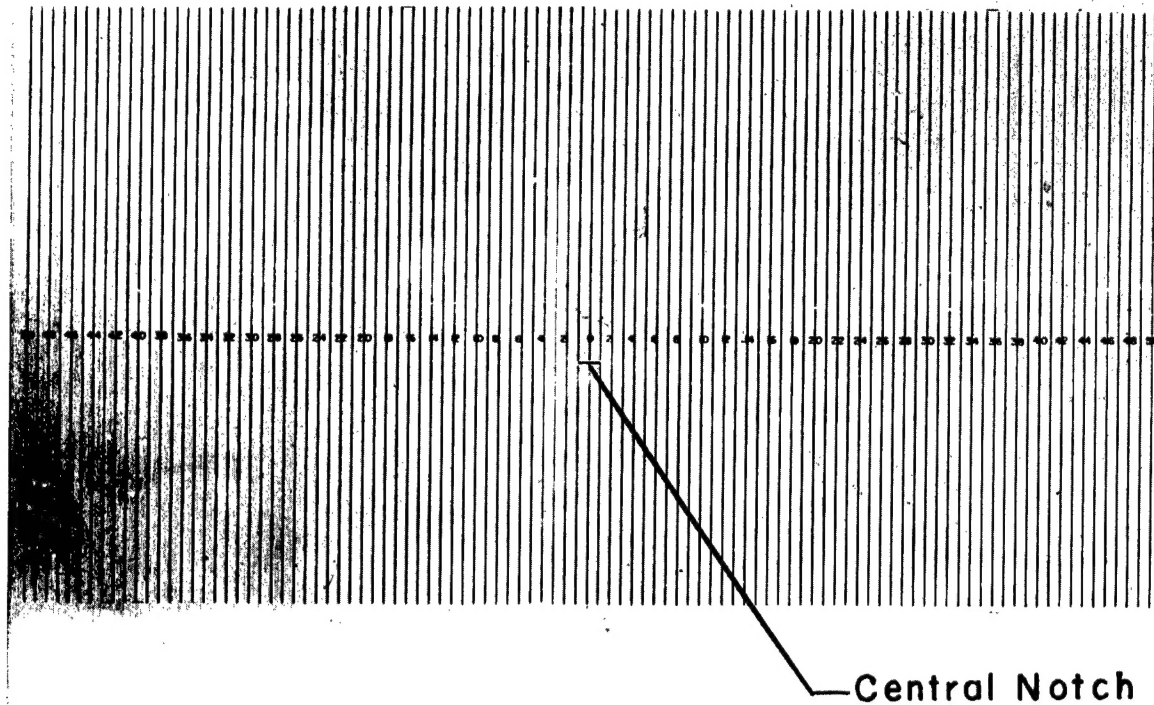


Figure 1.- Specimen configuration for crack propagation studies.

Testing Equipment

Three axial-load fatigue testing machines were employed in this investigation. A 20 000-pound (89-kN) capacity subresonant fatigue machine (ref. 3) having an operating frequency of 1800 cpm (30 Hz) was used for tests expected to last more than 1 000 000 cycles. A 100 000-pound (445-kN) capacity hydraulic fatigue machine which applied loads at a rate of 1200 cpm (20 Hz) was employed in tests expected to last from 10 000 to 1 000 000 cycles. A combination hydraulic and subresonant fatigue testing machine (ref. 4) capable of applying loads up to 132 000 pounds (587 kN) hydraulically or 110 000 pounds (489 kN) subresonantly was used as the needs for testing dictated. The operating frequencies were 40 to 60 cpm (0.7 to 1 Hz) for the hydraulic unit, and approximately 820 cpm (14 Hz) for the subresonant unit.

In all tests, loads were monitored by measuring the output of a bridge circuit whose active elements were wire-resistance strain gages. These gages were fixed to weigh bars through which the load was transmitted to a specimen. Monitoring precision was approximately ± 1 percent.

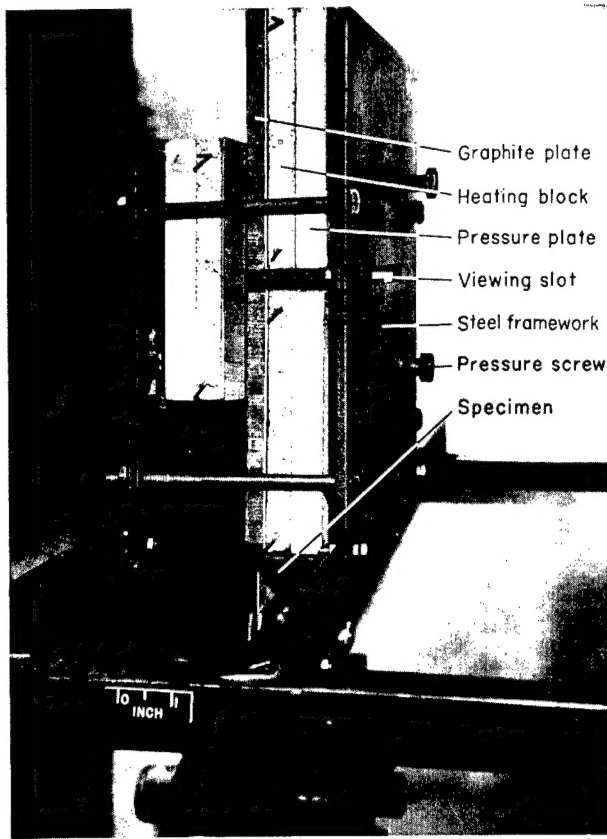


L-63-4299.1
Figure 2.- Grid used to mark intervals in crack path. Grid spacing is 0.05 inch
(1.27 mm).

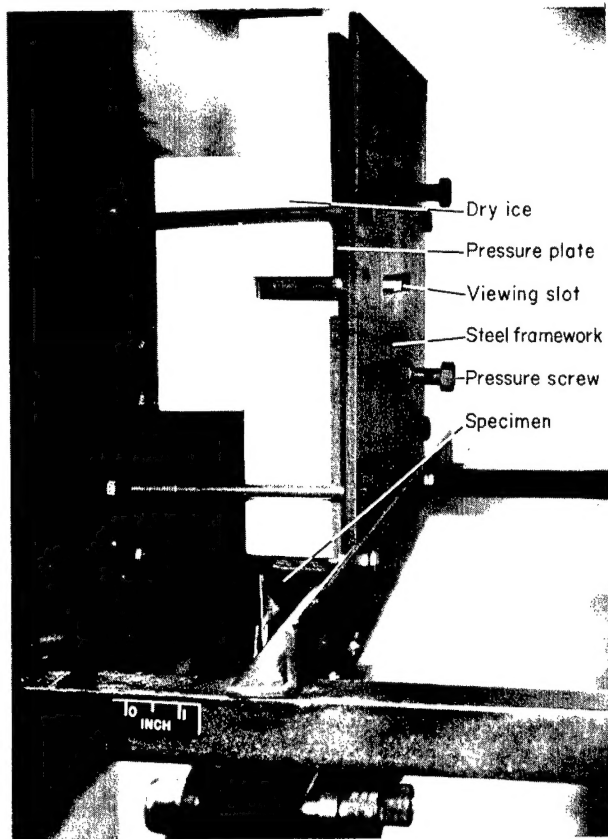
The apparatus used in the elevated-temperature tests (fig. 3) consisted of three heating units and a steel framework which held the heating units in contact with the specimen. The heating units were composed of a 1/2-inch (1.27-cm) thick graphite plate, a ceramic block containing wire resistance heaters, and an insulating pressure plate. A machine screw was jammed against the insulating pressure plate to hold the heating unit in contact with the specimen surface. The screws were carefully tightened to insure thermal contact without introducing significant frictional forces. Two heating units were placed on the observation side of the specimen; one above and the other below the region of crack growth. A 1/2-inch (1.27-cm) gap was provided to insure an unobstructed view of the propagating crack. The third unit was located on the opposite surface immediately opposite the crack-growth region.

A control thermocouple was fixed in the expected crack path near the edge of the specimen. By using an edge control point, the temperature was found to vary $\pm 5^\circ$ F ($\pm 3^\circ$ K) across the specimen width. The temperature at a given point was found to vary $\pm 2^\circ$ F ($\pm 1^\circ$ K) during the course of the test. Temperature control was maintained in the elevated-temperature tests by a controller-recorder which regulated current flow through a saturable reactor. The controller operated at 208 volts using 60-cycle single-phase ac power.

The equipment used in the -109° F (195° K) tests (fig. 4) consisted of three blocks of dry ice, the same steel framework used for the furnace, and an insulating cover box. The dry ice blocks were mounted in the steel framework



L-63-9528.2
Figure 3.- Elevated-temperature-test apparatus.



L-63-9529.2
Figure 4.- Cryogenic-temperature-test apparatus.

and held in contact with the specimen surface in the same manner as the heating units. Test temperature was governed by the sublimation temperature of the dry ice and was found to vary less than 5° F (3° K).

The entire cooling apparatus was isolated from circulating air drafts by the insulating cover box. This isolation was necessary in order to control the sublimation rate of the dry ice satisfactorily. The specimen surfaces were periodically sprayed with ethyl alcohol to prevent frost buildup in the crack-growth region.

Specimens were clamped between 3/8-inch (0.95-cm) thick aluminum guides (ref. 5) to prevent buckling and out-of-plane vibrations in all the room-temperature tests. Guides were also used in the elevated- and cryogenic-temperature tests in which compressive loadings were applied. In these latter tests, the heating or cooling units were placed directly against the guide plates and the specimen was heated or cooled by heat conduction through the guides. Good temperature control was maintained throughout these tests.

Specimen surfaces were lubricated with light oil in the room- and cryogenic-temperature tests and with dry molybdenum disulfide in the elevated-temperature tests. One side of the guide contained a 1/2-inch (1.27-cm) cutout across its width to allow visual observation of the crack path. A transparent plate was fitted into the guide cutout to prevent buckling of the specimen.

Test Procedure

Constant-amplitude axial-load fatigue tests were conducted at positive mean stresses of 40 ksi (276 MN/m^2) for AM 350, AM 367, and Inconel 718; 25 ksi (173 MN/m^2) for Ti-8Al-1Mo-1V; and 15 ksi (104 MN/m^2) for 2020-T6, RR-58 (clad), and 2024-T81 (clad). All stresses mentioned herein refer to the original net area of the specimen. Alternating stresses ranged from ± 60 to ± 5 ksi (± 414 to $\pm 30 \text{ MN/m}^2$) for AM 350, AM 367, and Inconel 718; ± 25 to ± 2 ksi (± 173 to $\pm 14 \text{ MN/m}^2$) for Ti-8Al-1Mo-1V; and ± 15 to ± 2 ksi (± 104 to $\pm 14 \text{ MN/m}^2$) for 2020-T6, RR-58 (clad), and 2024-T81 (clad). Mean and alternating loads were kept constant throughout each test.

Tests were conducted at 80° F (300° K) and -109° F (195° K) on all materials, at 550° F (561° K) on the stainless steels, titanium alloys, and the superalloy, and at 250° F (394° K) on the aluminum alloys. Specimens were tested at the same stress levels at all test temperatures in order to evaluate the effect of temperature on crack propagation.

The test data were obtained by observing the crack growth through 30 power microscopes while illuminating the specimen with stroboscopic light. The number of cycles required to propagate the crack to each grid line was recorded so that the rate of crack propagation could be determined. Tests were terminated when the cracks reached a predetermined crack length, and the specimens were reserved for the subsequent residual static-strength investigation reported in reference 6.

RESULTS AND DISCUSSION

The crack-propagation-test results are presented in table IV which gives the number of cycles required to propagate a crack from a half length of 0.15 inch (0.38 cm). The number of cycles given in table IV, and in figures 5 to 12, is the mean number of cycles required to grow cracks of equal length on both sides of the central starter notch. The numbers of cycles are referenced from a half crack length of 0.15 inch (0.38 cm) because at this length the fatigue crack growth is no longer influenced by the starter notch (ref. 7).

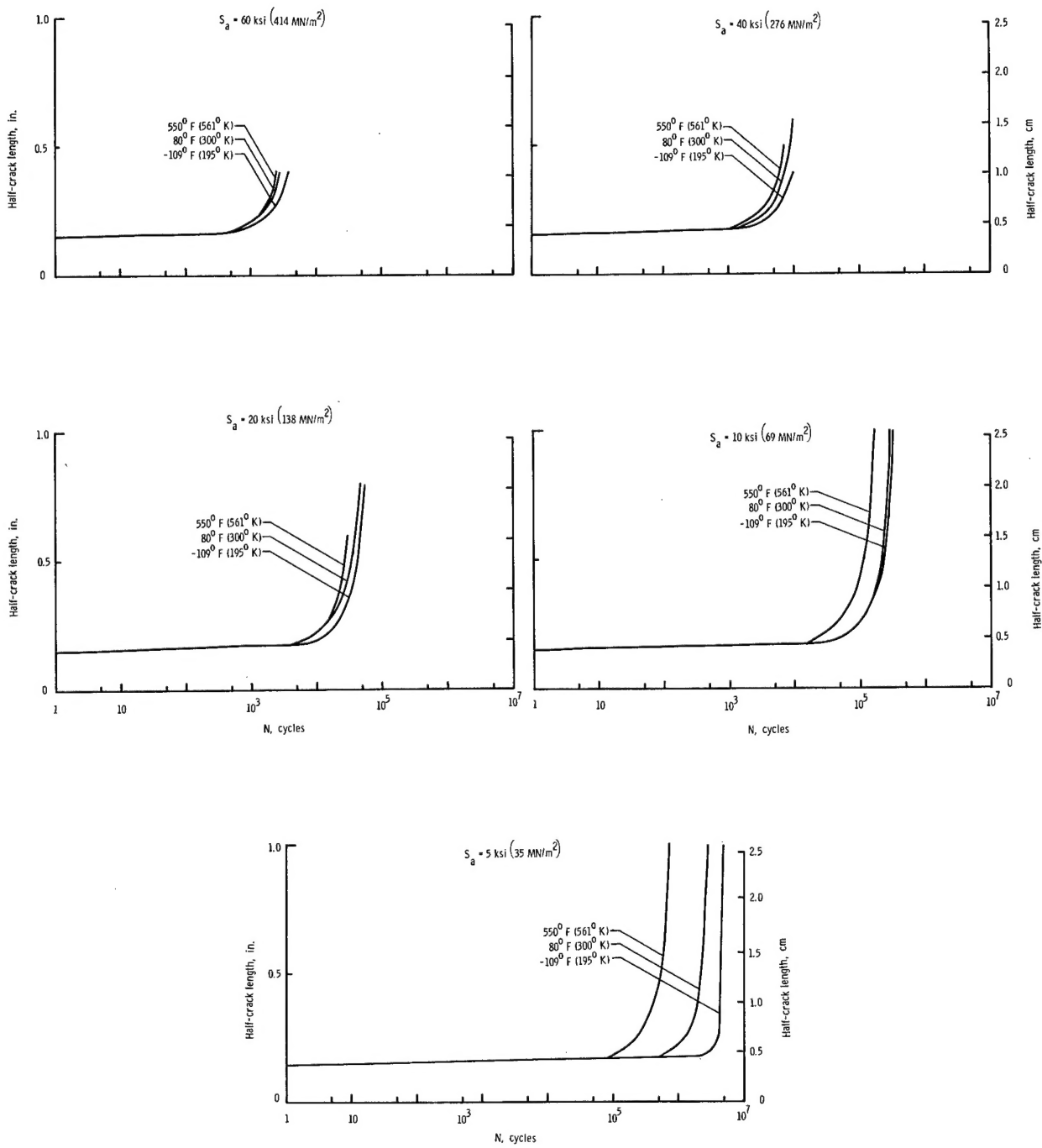


Figure 5.- Fatigue-crack-propagation curves for Inconel 718. $S_m = 40$ ksi (276 MN/m^2).

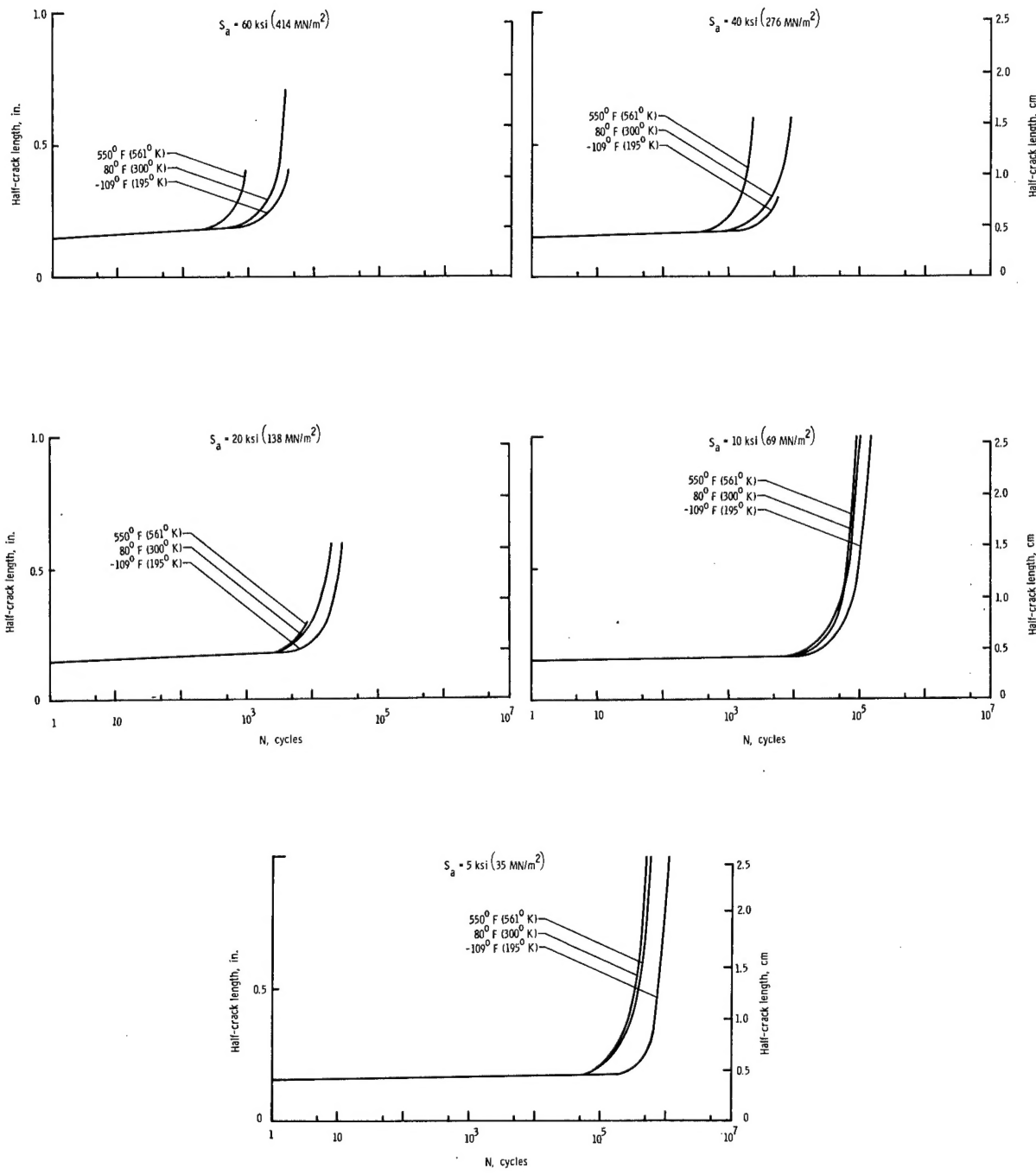


Figure 6.- Fatigue-crack-propagation curves for AM 350 (CRT). $S_m = 40$ ksi (276 MN/m^2).

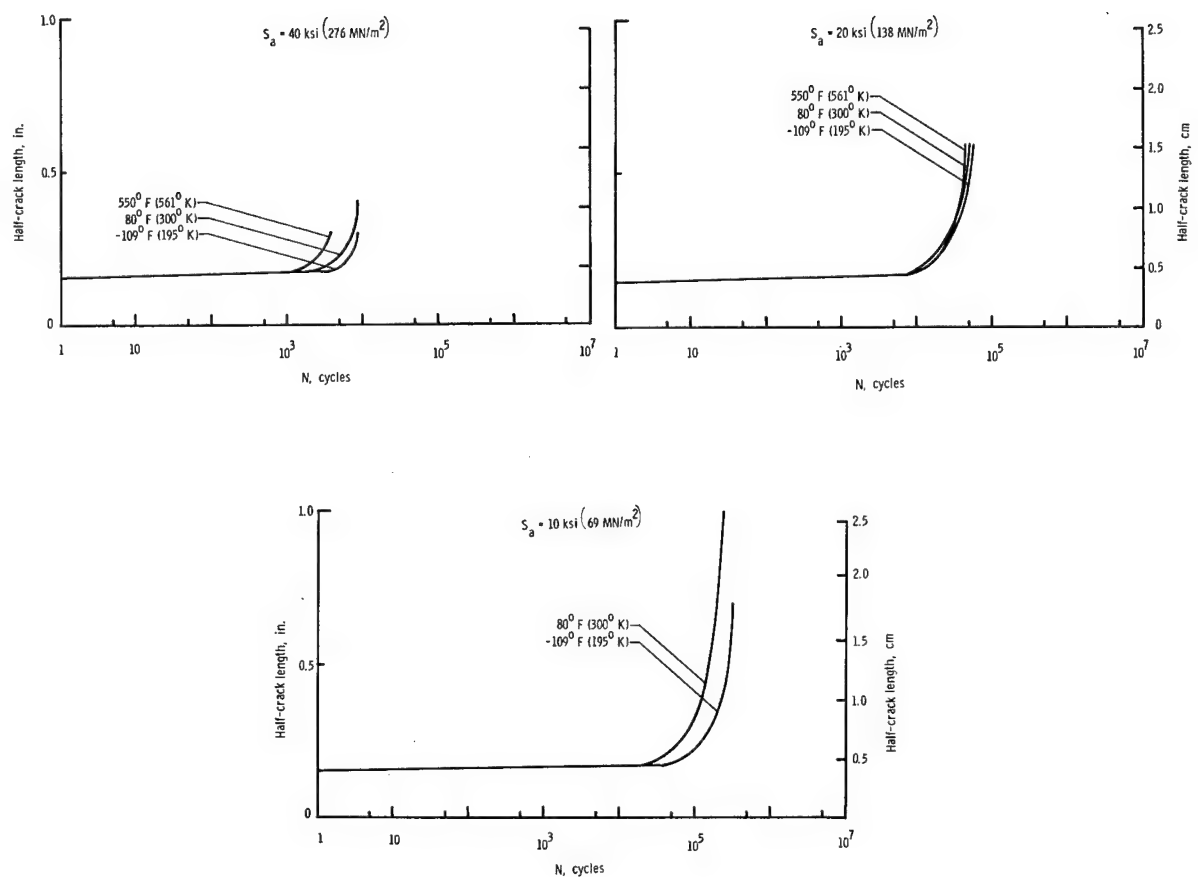


Figure 7.- Fatigue-crack-propagation curves for AM 367. $S_m = 40 \text{ ksi} (276 \text{ MN/m}^2)$.

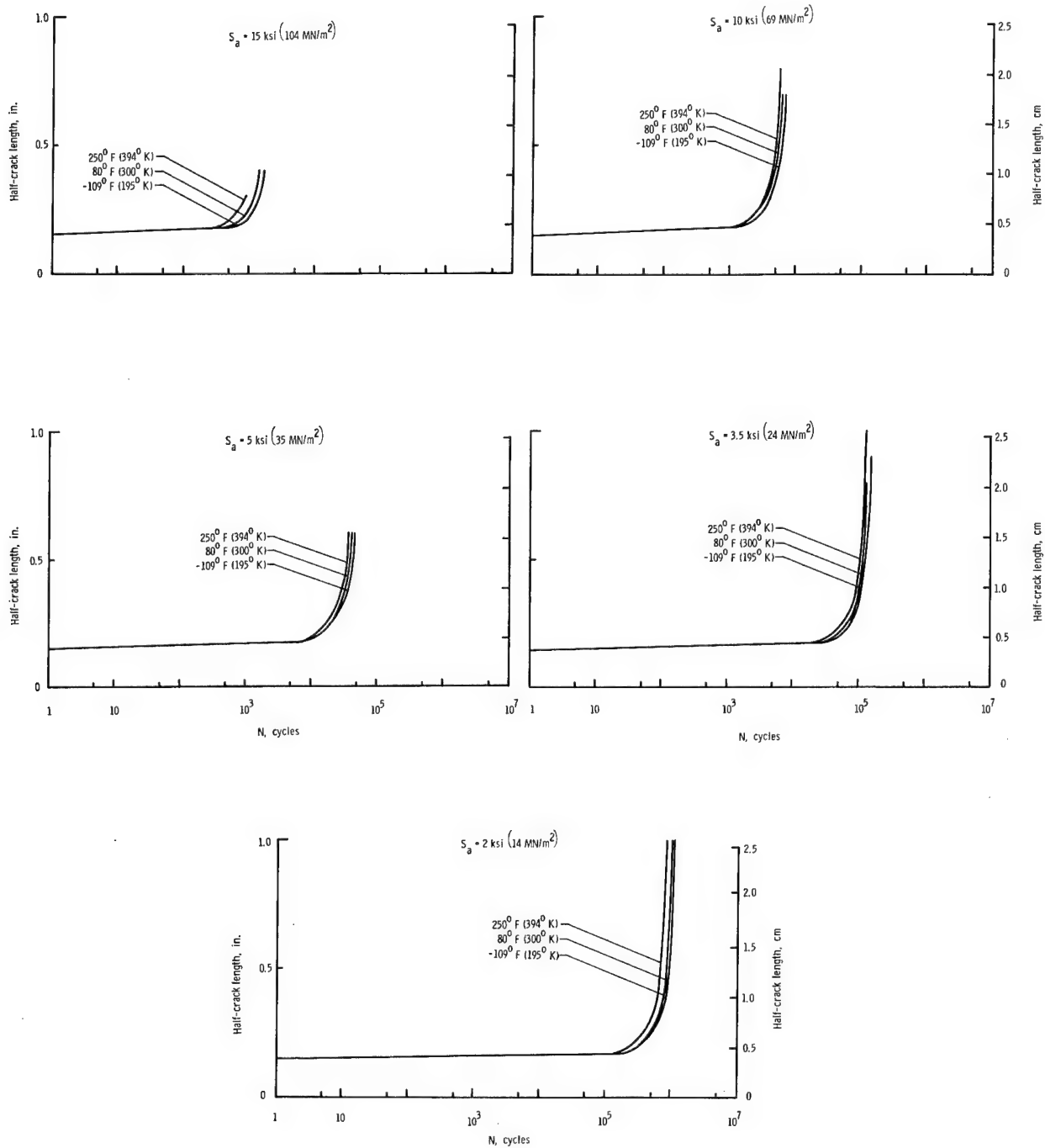


Figure 8.- Fatigue-crack-propagation curves for 2024-T81 (clad). $S_m = 15 \text{ ksi}$ (104 MN/m^2).

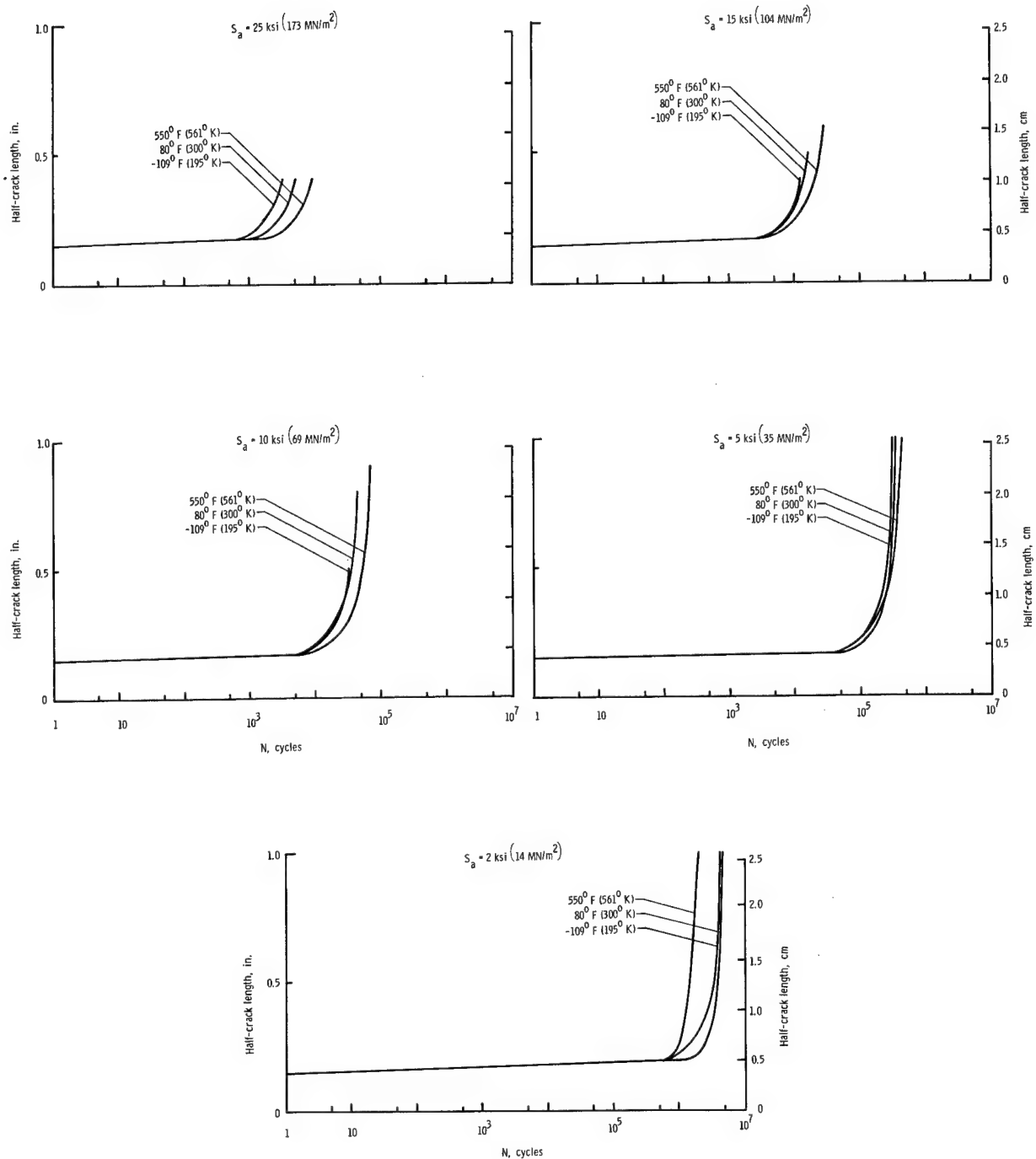


Figure 9--Fatigue-crack-propagation curves for Ti-8Al-1Mo-1V (duplex annealed).
 $t = 0.050$ inch (1.270 mm); $S_m = 25 \text{ ksi}$ (173 MN/m^2).

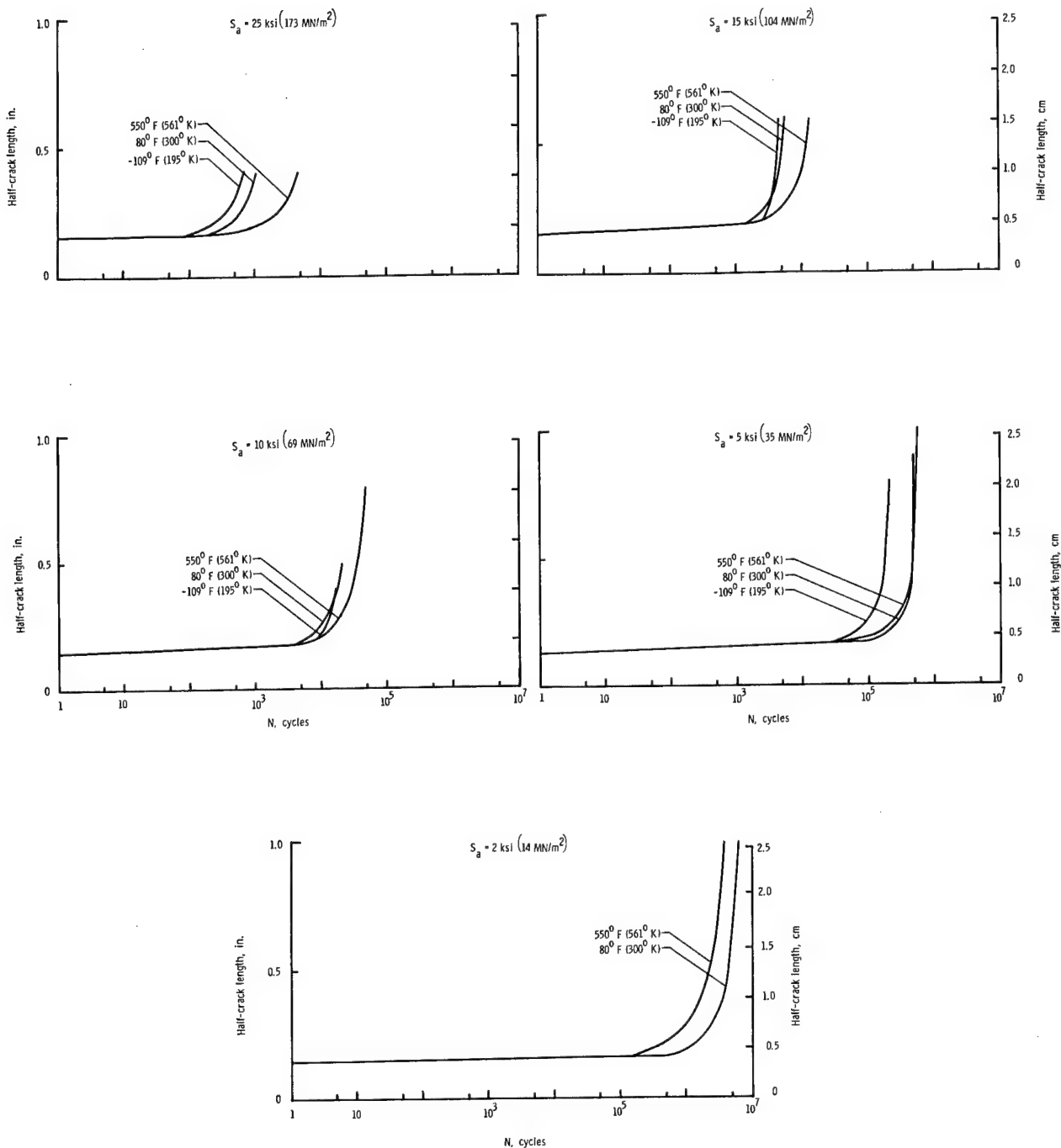


Figure 10.- Fatigue-crack-propagation curves for Ti-8Al-1Mo-1V (duplex annealed).
 $t = 0.250 \text{ inch (6.350 mm)}$; $S_m = 25 \text{ ksi (173 MN/m}^2\text{)}$.

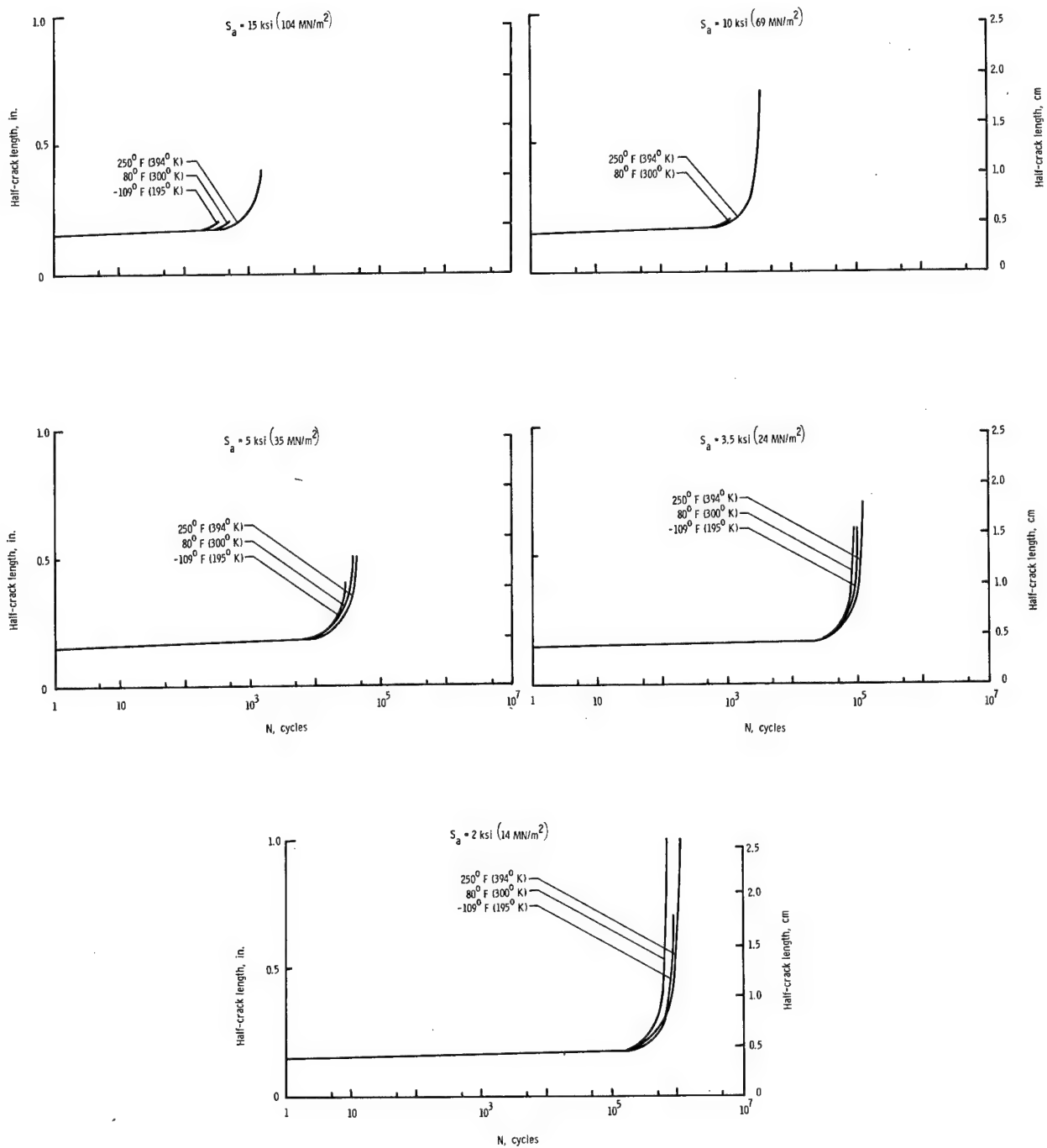


Figure 11.- Fatigue-crack-propagation curves for 2020-T6. $S_m = 15 \text{ ksi} (104 \text{ MN/m}^2)$.

| Temperature Effect

The effect of temperature on crack growth was determined by comparison of the crack propagation curves from tests at room, elevated, and cryogenic temperatures. The crack-growth curves for Inconel 718, AM 350, AM 367, and 2024-T81 (clad) (figs. 5, 6, 7, and 8, respectively) show almost without exception that the higher the temperature, the more rapidly fatigue cracks propagated. A similar change of crack-growth resistance with temperature was found for the stainless steels and a superalloy tested in the previous crack-growth investigation (ref. 1). The loss of resistance to fatigue crack growth with increasing temperature may be attributed to the normal deterioration of properties at elevated temperature.

The crack-growth curves for both thicknesses of Ti-8Al-1Mo-1V (duplex annealed) and for 2020-T6 (figs. 9, 10, and 11, respectively) indicate that fatigue cracks generally grow most slowly at elevated temperature, and most rapidly at cryogenic temperature. In most instances, however, the differences between the crack-growth curves were small. The titanium alloys tested in reference 1 were also found to be slightly more resistant to crack growth at elevated temperature.

The fatigue-crack-growth curves for the RR-58 (clad) (fig. 12) indicate no consistent variation of crack-growth resistance with temperature. At the higher stress levels the RR-58 (clad) showed the greatest resistance at room temperature, while at the lower stress levels the resistance was greatest at 250° F (394° K).

| Crack-Growth Resistance of Materials

The relative crack-growth resistance of the various materials was determined by comparing plots of the rates of fatigue crack growth against the ratio of the alternating to the mean stress (i.e., the stress ratio). The lower the rate of crack growth for a given stress ratio, the greater the resistance of the material to fatigue crack growth. The crack-growth rates were determined graphically by taking the slopes of the fatigue-crack-growth curves (on a linear plot) at different crack lengths. Figures 13, 14, and 15 show the rate plotted against stress ratio for the elevated-, room-, and cryogenic-temperature tests, respectively. The rates shown in these three figures are for a half crack length a of 0.40 inch (1.02 cm). The materials generally maintained the same relative positions at other crack lengths.

The mean stresses at which the comparisons in figures 13 to 15 were made are approximately one-fifth of the ultimate tensile strength of the materials. The mean stress-density ratios for the materials are also approximately equal.

At elevated temperature (fig. 13), the thin titanium sheet showed the greatest resistance to crack growth, followed by Inconel 718, and the thick titanium plate. The results of tests on AM 367 indicate good crack-growth resistance at elevated temperature, but only a small number of tests were conducted. Fatigue-crack-growth rates in the 2020-T6, RR-58 (clad), 2024-T81 (clad), and AM 350 were relatively high.

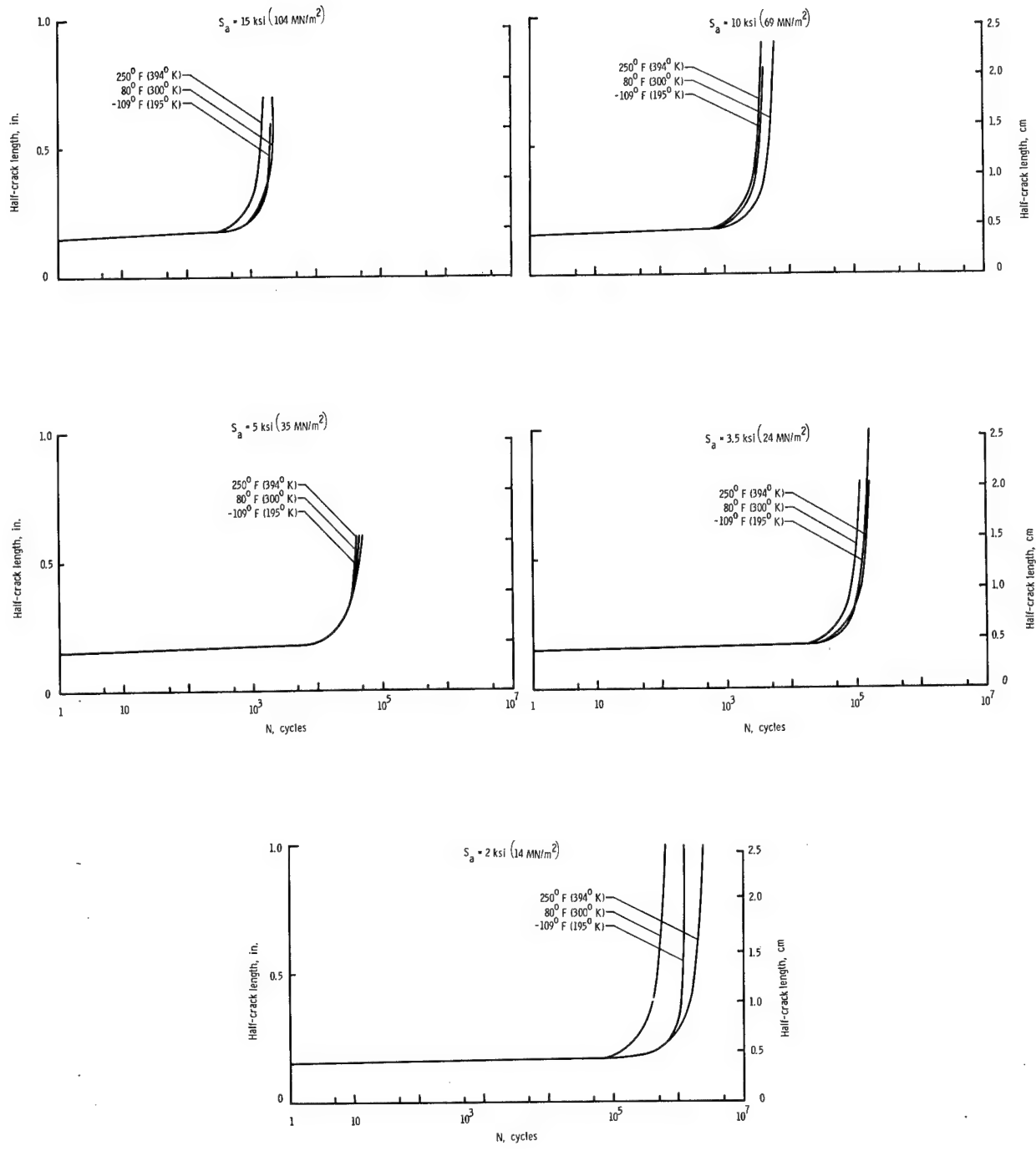


Figure 12.- Fatigue-crack-propagation curves for RR-58 (clad). $S_m = 15$ ksi (104 MN/m^2).

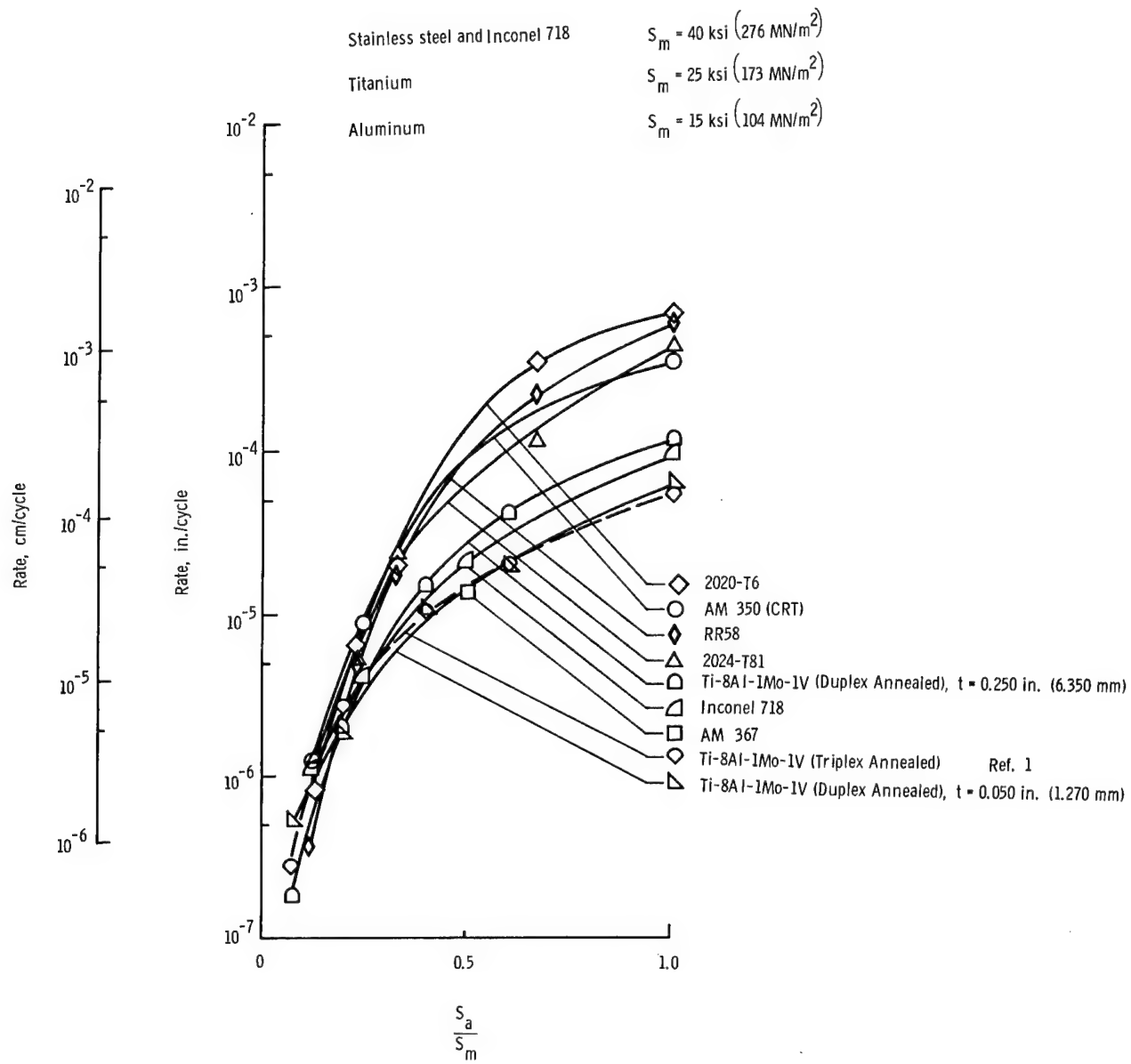


Figure 13.- Fatigue-crack-propagation rate as a function of the ratio of alternating to mean stress at elevated temperature ($250^\circ \text{ F } (394^\circ \text{ K})$ for the aluminums, $550^\circ \text{ F } (561^\circ \text{ K})$ for all others) for a half crack length a of 0.40 inch (1.02 cm).

Data from tests at $550^\circ \text{ F } (561^\circ \text{ K})$ and at $250^\circ \text{ F } (394^\circ \text{ K})$ are compared directly in figure 13 in order to evaluate the relative efficiencies of the various materials at the approximate elevated temperature extremes to which the materials might be subjected in supersonic aircraft.

At room temperature (fig. 14), Inconel 718 and AM 367 exhibited the lowest fatigue-crack-growth rates followed by AM 350 and the thin titanium sheet. The crack-growth rates again were quite high for the three aluminum alloys and also

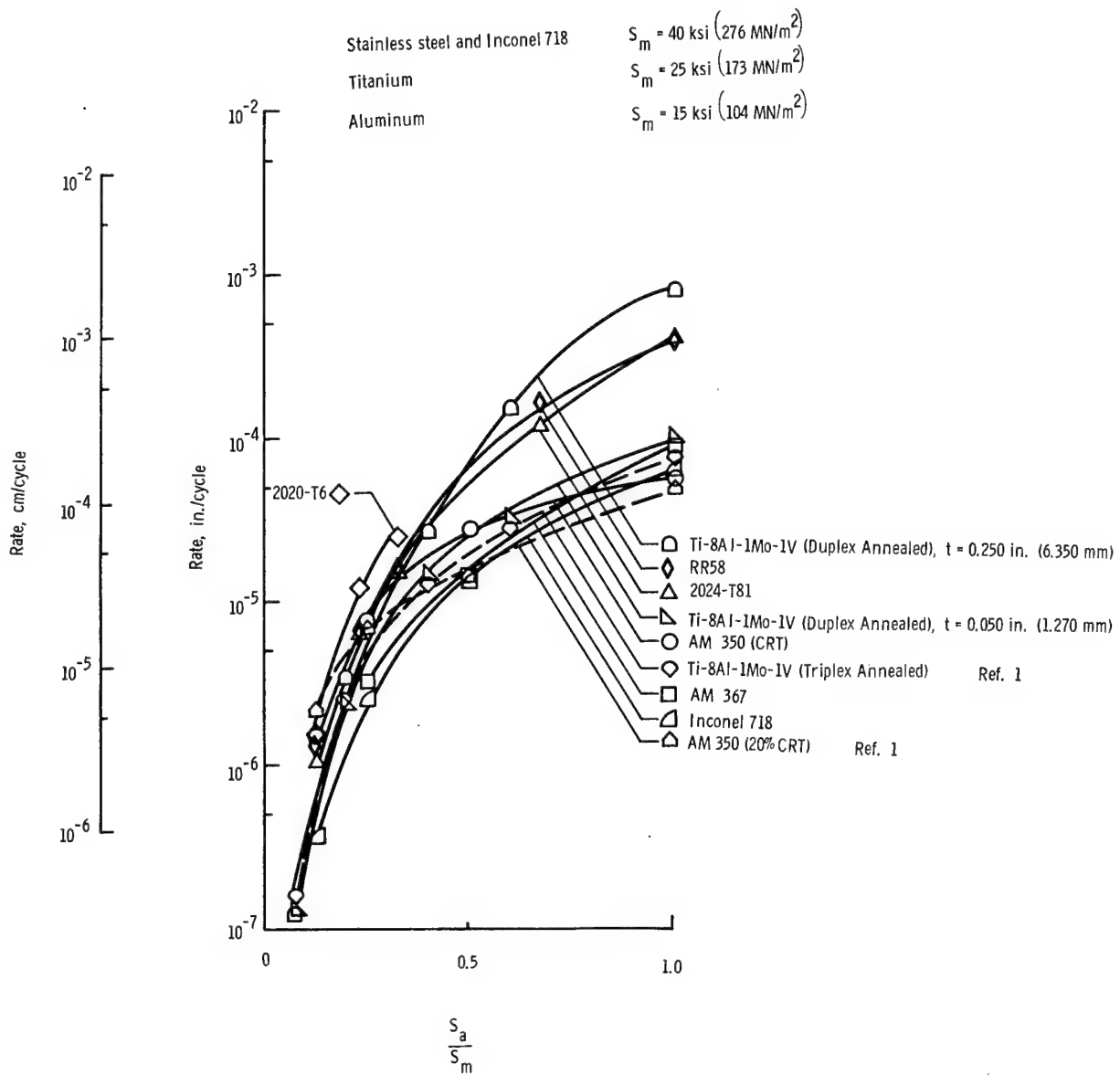


Figure 14.- Fatigue-crack-propagation rate as a function of the ratio of alternating to mean stress at 80° F (300° K) for a half crack length a of 0.40 inch (1.02 cm).

for the thick titanium plate. The AM 367 and Inconel 718 (fig. 15) also showed the greatest resistance to fatigue crack growth at cryogenic temperature. The AM 350 and the thin titanium sheet followed. The three aluminum alloys and the thick titanium plate were once again the least resistant materials tested.

Thus, it appears that over the temperature range of the investigation, the Inconel 718 and the AM 367 exhibited the greatest overall resistance to fatigue crack growth. It should be remembered, however, that a somewhat smaller quantity of data was obtained on the AM 367. It further appears that the crack-growth resistance of the thick titanium plate is considerably lower than the resistance of the thin sheet. This lower crack-growth resistance may result

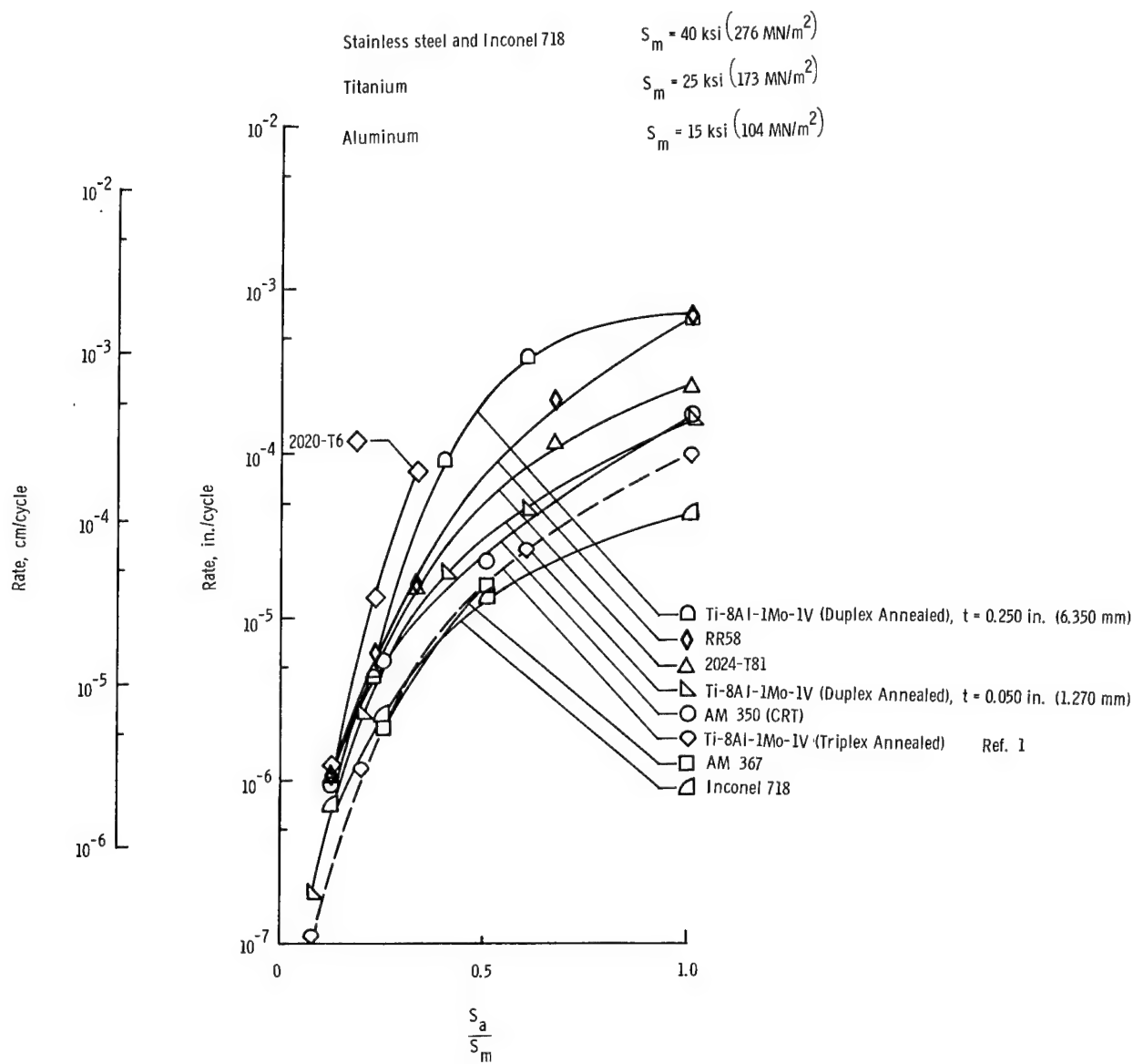


Figure 15.- Fatigue-crack-propagation rate as a function of the ratio of alternating to mean stress at -109° F (195° K) for a half crack length a of 0.40 inch (1.02 cm).

from a tri-axial stress state inherent in the thicker material. In this state, the plastic deformation in the material ahead of the crack tip is partially restrained by the large bulk of elastic material surrounding the plastic zone. This restraint of plastic flow causes the stresses in this plastic zone to increase to a higher level than would be possible if plastic flow could occur readily, as in thin sheet materials. These higher stresses could promote a faster rate of fatigue crack growth. The difference between crack-growth resistance of the thick and the thin titanium material could also have resulted from the different amounts of working to which the material was subjected in processing.

For purposes of comparison, the crack-growth-rate against stress-ratio curves for sheet Ti-8Al-1Mo-1V (triplex annealed) titanium alloy, and AM 350 (20% CRT) stainless steel, which showed the greatest crack-growth resistance in the previous investigation (ref. 1), have been included (dashed curves) with the test data reported herein. Inspection of figures 13, 14, and 15 indicates that for the entire spectrum of materials tested, the sheet Ti-8Al-1Mo-1V titanium alloy in either the duplex- or triplex-annealed condition has the greatest resistance to fatigue crack growth at elevated temperature. At the room and cryogenic temperatures, Inconel 718 generally appeared to be most resistant. The AM 367 also exhibited relatively good crack-growth characteristics at all three test temperatures.

The data for the triplex-annealed titanium alloy has been included at all three test temperatures to show the effect of the different annealing processes on the crack-growth resistance. The curves indicate that at elevated temperature the crack-growth characteristics of the triplex-annealed alloy are approximately equal to those of the duplex-annealed alloy. At the room and cryogenic temperatures, the triplex-annealed alloy is generally more resistant to crack growth than is the duplex-annealed alloy.

CONCLUSIONS

The following conclusions were drawn from the investigation of the fatigue-crack-growth characteristics of seven materials considered for structural applications in supersonic aircraft design. Tests were conducted at temperatures of -109° F (195° K), 80° F (300° K), and either 550° F (561° K) or 250° F (394° K) depending upon the material.

1. The higher the temperature the more rapidly fatigue cracks propagated in AM 350 (CRT) and AM 367 stainless steel, Inconel 718 superalloy, and 2024-T81 (clad) aluminum alloy. Cracks were found to grow more rapidly as the temperature decreased in the Ti-8Al-1Mo-1V (duplex annealed) titanium alloy and the 2020-T6 aluminum alloy. These conclusions concur in general with those presented in NASA Technical Note D-2331. The RR-58 (clad) aluminum alloy exhibited no consistent variation of crack-growth resistance with temperature. P. 20
2. The superalloy Inconel 718 exhibited the greatest overall resistance to fatigue crack growth. The 0.050-inch (1.27-mm) thick Ti-8Al-1Mo-1V (duplex annealed) sheet material was the most resistant to crack growth at elevated temperature followed by Inconel 718. The Inconel 718 showed the greatest resistance to crack propagation at room and cryogenic temperatures. A limited number of tests on AM 367 indicated this material has good resistance to crack growth, but only a small number of tests were conducted.
3. The fatigue-crack-growth resistance of the 0.250-inch (6.35-mm) thick Ti-8Al-1Mo-1V (duplex annealed) titanium alloy was considerably lower than the resistance of the 0.050-inch (1.27-mm) thick material. This lower resistance in the thicker material may result from a tri-axial stress state, or from a difference in the cold working.

4. For the test conditions used, the crack-growth resistance of the 2020-T6, RR-58 (clad), and 2024-T81 (clad) aluminum alloys was relatively poor over the entire temperature range.

5. Comparison of the crack-growth-rate with stress-ratio curves for the sheet Ti-8Al-1Mo-1V (duplex annealed) with similar curves for sheet Ti-8Al-1Mo-1V (triplex annealed) obtained in a previous investigation (TN D-2331), shows that crack-growth characteristics are quite similar at elevated temperature. However, at the room and cryogenic temperatures the triplex-annealed alloy was generally more crack-growth resistant than the duplex-annealed alloy.

Langley Research Center,
National Aeronautics and Space Administration,
Langley Station, Hampton, Va., January 6, 1965.

REFERENCES

1. Hudson, C. Michael: Fatigue-Crack Propagation in Several Titanium and Stainless-Steel Alloys and One Superalloy. NASA TN D-2331, 1964.
2. Mechtly, E. A.: The International System of Units - Physical Constants and Conversion Factors. NASA SP-7012, 1964.
3. Grover, H. J.; Hyler, W. S.; Kuhn, Paul; Landers, Charles B.; and Howell, F. M.: Axial-Load Fatigue Properties of 24S-T and 75S-T Aluminum Alloy as Determined in Several Laboratories. NACA Rept. 1190, 1954. (Supersedes NACA TN 2928.)
4. Hudson, C. Michael; and Hardrath, Herbert F.: Investigation of the Effects of Variable-Amplitude Loadings on Fatigue Crack Propagation Patterns. NASA TN D-1803, 1963.
5. Brueggeman, W. C.; and Mayer, M., Jr.: Guides for Preventing Buckling in Axial Fatigue Tests on Thin Sheet-Metal Specimens. NACA TN 931, 1944.
6. Figge, I. E.: Residual Strength of Alloys Potentially Useful in Supersonic Aircraft. NASA TN D-2613, 1965.
7. McEvily, Arthur J., Jr.; and Illig, Walter: The Rate of Fatigue-Crack Propagation in Two Aluminum Alloys. NACA TN 4394, 1958.
8. Weiss, V.; and Sessler, J. G., eds.: Aerospace Structural Metals Handbook. Volume II - Non-Ferrous Alloys. ASD-TDR-63-741, Vol. II, U.S. Air Force, Mar. 1963.

TABLE I.- AVERAGE TENSILE PROPERTIES OF MATERIALS TESTED

[Grain direction longitudinal]

Temperature		Ultimate tensile strength		Yield strength (0.2% offset)		Modulus of elasticity		Elongation, percent 2-in. (5.08-cm) gage length	Number of tests
°F	°K	ksi	MN/m ²	ksi	MN/m ²	ksi	GN/m ²		
AM 367									
-109 80 550	195 300 561	266.0 243.4 206.1	1835 1680 1422	263.7 242.0 201.3	1820 1670 1389	31.4×10^3 30.7 20.1	217 212 139	5.0 4.2 3.8	3 3 3
AM 350 (CRT)									
-109 80 550	195 300 561	266.3 223.4 197.8	1838 1542 1365	222.0 217.5 184.5	1532 1501 1273	28.6×10^3 27.8 22.5	197 192 155	20.7 16.2 3.0	3 3 3
Inconel 718									
-109 80 550	195 300 561	195.0 193.7 172.1	1346 1337 1187	161.2 162.2 144.7	1112 1119 998	27.8×10^3 27.8 26.8	192 192 185	28.0 23.3 19.0	3 3 4
Ti-8Al-1Mo-1V (duplex annealed); t = 0.050 inch (1.27 mm)									
-109 80 550	195 300 561	178.0 152.0 115.5	1228 1049 797	162.7 133.6 93.7	1123 922 647	17.7×10^3 18.3 14.1	121 126 97	15.3 12.5 12.0	3 3 3
Ti-8Al-1Mo-1V (duplex annealed); t = 0.250 inch (6.35 mm)									
-109 80 550	195 300 561	157.5 137.4 113.8	1087 948 785	145.6 120.0 85.8	1005 828 592	16.9×10^3 14.8 13.3	117 102 92	11.0 17.3 16.5	3 3 2
2020-T6									
-109 80 250	195 300 394	88.3 81.8 68.8	609 564 475	82.4 77.5 64.0	569 535 442	12.4×10^3 11.3 9.7	86 78 67	7.7 8.8 9.0	3 4 3
2024-T81 (clad)									
-109 80 250	195 300 394	69.0 63.2 59.3	476 436 409	62.2 57.6 53.3	429 397 368	8.8×10^3 9.5 8.4	61 66 58	7.0 7.2 7.5	3 3 3
RR-58 (clad)									
-109 80 250	195 300 394	64.6 59.2 54.0	445 408 372	58.8 54.6 51.3	405 377 354	10.4×10^3 10.0 10.5	72 69 72	8.3 7.0 7.3	3 3 3

TABLE II.-- NOMINAL CHEMICAL COMPOSITION OF MATERIALS TESTED

Element	AM 367, percent	AM 350, percent	Inconel 718, percent	Ti-8Al-1Mo-1V, percent	2020-T6, percent	2024-T81 (clad), percent	RR-58 (clad), percent
C	0.021	0.08 to 0.12	0.10 max	0.08 max	0.30 to 0.80	0.30 to 0.90	
Mn	0.024	0.50 to 1.25	0.50 max				
P	0.002	0.040 max					
S	0.009	0.030 max					
Si	0.080	0.50 max	0.75 max				
Ni	3.40	4.00 to 5.00	50.0 to 55.0				
Cr	14.25	16.00 to 17.00	17.0 to 21.0				
Mo	1.99	2.50 to 3.25	2.80 to 3.30	0.75 to 1.25			
V				0.75 to 1.25			
Al	0.03	0.20 to 1.00	7.50 to 8.50				
N			0.05 max				
H			0.015 max				
Ti	0.35	0.30 to 1.30	Balance	0.10 max			0.1
Fe	Balance	Balance	0.30 max	0.40 max			1.0
Co	15.44						
Cu + Ta		4.50 to 5.75		4.0 to 5.0	3.8 to 4.9	2.5	
Li				0.9 to 1.7			
Mg				0.03 max	1.2 to 1.8		
Zn				0.25 max	0.25 max	1.5	
Cd				0.10 to 0.35			

TABLE III.-- MATERIAL HEAT TREATMENTS

Material	Condition	Heat treatment
AM 367	-----	Annealed 1400° F (1033° K), quench to -100° F (200° K) for 16 hr, aged 8 hr at 850° F (727° K), air cool
AM 350	CRT	20% cold rolled, tempered 3 to 5 min at 930° F (772° K), air cool
Inconel 718	-----	Annealed 1325° F (993° K) for 8 hr, furnace cool 20° F/hr to 1150° F (894° K), air cool
Ti-8Al-1Mo-1V	Duplex annealed	1450° F (1061° K) for 8 hr, furnace cool, 1450° F (1061° K) for 15 min, air cool
RR-58 (clad)	Fully heat treated to specification DTD 5070 A	5 min to 1 hr at 525° C to 530° C (798° K to 803° K), depending on gage, quench in cold water, 10 to 30 hr at 190° C ± 5° C (463° K ± 5° K)
2020	T6	See reference 8
2024 (clad)	T81	See reference 8

TABLE IV.— MEAN NUMBER OF CYCLES REQUIRED TO EXTEND CRACKS FROM A HALF-LENGTH OF 0.15 INCH (0.38 CM)

^aCrack initiated at Sa of 10 ksi (69 MN/m²) to expedite testing.
^bCrack initiated at Sa of 5 ksi (35 MN/m²) to expedite testing.

Crack initiated at S_a of 5 ksi (35 MN/m^2) to expedite testing.

TABLE IV. - MEAN NUMBER OF CYCLES REQUIRED TO EXTEND CRACKS FROM A HALF-LENGTH OF 0.15 INCH (0.38 cm) - Concluded

Temperature	S_a	Number of cycles required to propagate a crack from a half length a of 0.15 inch (0.38 cm) to a length a of -									
		0.40 in. (1.016 cm)	0.50 in. (1.270 cm)	0.50 in. (1.270 cm)	0.60 in. (1.524 cm)	0.70 in. (1.778 cm)	0.80 in. (2.032 cm)	0.90 in. (2.286 cm)	1.00 in. (2.540 cm)	1.20 in. (3.048 cm)	1.40 in. (3.556 cm)
80	300 15 104	1 750	3 700	4 900	11 300	31 000	38 500	42 000	45 000	310 000	330 000
80	300 10 69	1 300	19 500	28 000	200 000	240 000	265 000	285 000	300 000	320 000	350 000
80	300 5 24	75	25	290 000	2 800 000	3 280 000	3 700 000	4 020 000	4 260 000	4 500 000	4 770 000
80	300 2 14	660 000	1 800 000	2 645 000	6 500	8 900	20 900	25 600	29 400	320 000	350 000
550	561 25	173	2 900	6 200	14 900	42 500	51 000	58 000	64 000	69 500	74 000
550	561 15	104	13 500	31 500	74 000	181 000	208 000	248 000	300 000	367 000	409 000
550	561 5	35	708 000	1 018 000	1 298 000	1 428 000	1 563 000	1 685 000	1 788 000	1 868 000	1 943 000
-109	195 25	173	1 075	3 275	3 025	10 500	13 500	16 500	28 000	32 600	427 000
-109	195 15	104	4 900	10 200	14 500	21 000	21 000	21 000	282 000	304 000	2 048 000
-109	195 10	69	9 800	21 000	21 000	21 000	21 000	21 000	282 000	304 000	2 163 000
-109	195 5	35	97 000	195 000	219 000	271 000	272 000	272 000	3 512 000	3 742 000	2 123 000
-109	195 2	14	1 502 000	1 502 000	1 502 000	1 502 000	1 502 000	1 502 000	1 502 000	1 502 000	1 502 000
80	300 15 104	500	1 250	27 500	33 000	36 000	39 500	42 000	45 000	48 000	51 000
80	300 10 69	11 500	58 000	67 500	79 500	86 500	92 000	98 500	105 000	112 000	119 000
80	300 5 24	25	288 000	460 000	560 000	610 000	660 000	710 000	760 000	810 000	860 000
80	300 2 14	b2	354	104	700	1 200	1 450	2 200	3 200	3 400	3 450
250	394 25	15	1 500	2 400	2 900	37 500	37 500	40 500	104 000	128 000	128 000
250	394 10	69	14 500	30 000	35 000	35 000	35 000	35 000	117 000	128 000	128 000
250	394 5	35	14 500	45 000	63 000	63 000	63 000	63 000	770 000	920 000	920 000
250	394 b2	24	290 000	340	340	340	340	340	770 000	870 000	870 000
-109	195 15	104	69	11 900	26 100	26 100	27 900	27 900	27 900	27 900	27 900
-109	195 5	24	39 000	65 000	76 000	76 000	76 000	76 000	76 000	76 000	76 000
-109	195 b2	14	345 000	345 000	345 000	345 000	345 000	345 000	345 000	345 000	345 000
80	300 15 104	640	1 340	1 670	1 670	1 670	1 670	1 670	1 670	1 670	1 670
80	300 10 69	1 600	3 650	4 850	5 600	5 600	5 600	5 600	5 600	5 600	5 600
80	300 5 24	25	12 000	26 000	34 000	40 000	46 000	52 000	58 000	64 000	70 000
80	300 2 14	b2	354	40 000	83 000	103 000	103 000	103 000	103 000	103 000	103 000
250	394 15	104	130	1 600	3 400	890	1 030	1 030	1 030	1 030	1 030
250	394 10	69	1 600	3 400	4 500	5 200	5 200	5 200	5 200	5 200	5 200
250	394 5	35	1 600	10 000	21 500	27 500	31 500	31 500	31 500	31 500	31 500
250	394 b2	24	31 000	71 000	96 000	110 000	110 000	110 000	110 000	110 000	110 000
250	394 3.5	5	230 000	475 000	580 000	650 000	650 000	650 000	650 000	730 000	730 000
250	394 1.5	14	895	1 725	2 250	5 500	6 100	6 600	6 900	759 000	759 000
-109	195 25	104	104	2 100	4 200	5 500	10 000	13 000	14 800	141 000	825 000
-109	195 10	69	12 000	35 000	68 000	112 000	129 000	140 000	148 000	158 000	845 000
-109	195 5	35	46 000	66 000	88 000	112 000	112 000	112 000	815 000	922 000	922 000
-109	195 b2	14	265 000	600 000	740 000	815 000	815 000	815 000	815 000	922 000	922 000
80	300 15 104	660	1 400	1 750	1 750	1 750	1 750	1 750	1 750	1 750	1 750
80	300 10 69	1 510	3 270	37 000	42 000	42 000	42 000	42 000	42 000	42 000	42 000
80	300 5 24	24	28 000	63 000	81 000	94 000	103 000	103 000	103 000	103 000	103 000
80	300 2 14	b2	138	290 000	360 000	360 000	440 000	440 000	510 000	510 000	510 000
250	394 15	104	470	1 080	2 120	2 720	3 000	3 300	3 450	3 500	3 520
250	394 10	69	1 600	14 000	37 000	41 000	41 000	41 000	41 000	41 000	41 000
250	394 5	35	45 000	145 000	149 000	159 000	159 000	168 000	168 000	171 000	171 000
250	394 b2	14	450 000	1 110 000	1 490 000	1 730 000	1 920 000	1 920 000	2 040 000	2 115 000	2 115 000
-109	195 15	104	740	1 500	1 780	1 910	1 910	1 910	1 980	2 040 000	2 185 000
-109	195 10	69	1 120	2 300	3 300	3 300	3 300	3 300	3 610	3 750	3 820
-109	195 5	35	13 500	22 500	38 000	43 000	43 000	43 000	46 700	47 700	48 700
-109	195 b2	14	48 000	90 000	112 000	127 000	127 000	127 000	137 000	144 000	151 000
-109	195 1.5	14	500 000	890 000	1 020 000	1 090 000	1 090 000	1 090 000	1 170 000	1 210 000	1 230 000

b Crack initiated by S_a of 5 ksi (35 MN/m^2) to expedite testing.

c Crack initiated at S_a of 3.5 ksi (24 MN/m^2) to expedite testing.

"The aeronautical and space activities of the United States shall be conducted so as to contribute . . . to the expansion of human knowledge of phenomena in the atmosphere and space. The Administration shall provide for the widest practicable and appropriate dissemination of information concerning its activities and the results thereof."

—NATIONAL AERONAUTICS AND SPACE ACT OF 1958

NASA SCIENTIFIC AND TECHNICAL PUBLICATIONS

TECHNICAL REPORTS: Scientific and technical information considered important, complete, and a lasting contribution to existing knowledge.

TECHNICAL NOTES: Information less broad in scope but nevertheless of importance as a contribution to existing knowledge.

TECHNICAL MEMORANDUMS: Information receiving limited distribution because of preliminary data, security classification, or other reasons.

CONTRACTOR REPORTS: Technical information generated in connection with a NASA contract or grant and released under NASA auspices.

TECHNICAL TRANSLATIONS: Information published in a foreign language considered to merit NASA distribution in English.

TECHNICAL REPRINTS: Information derived from NASA activities and initially published in the form of journal articles.

SPECIAL PUBLICATIONS: Information derived from or of value to NASA activities but not necessarily reporting the results of individual NASA-programmed scientific efforts. Publications include conference proceedings, monographs, data compilations, handbooks, sourcebooks, and special bibliographies.

Details on the availability of these publications may be obtained from:

SCIENTIFIC AND TECHNICAL INFORMATION DIVISION

NATIONAL AERONAUTICS AND SPACE ADMINISTRATION

Washington, D.C. 20546